

# Decarbonization and the time-delay between peak CO<sub>2</sub> emissions and concentrations

Ashwin K Seshadri

Divecha Centre for Climate Change, Centre for Atmospheric and Oceanic Sciences, Indian Institute of Science, Bangalore 560012. India.  
(ashwin@fastmail.fm)

## Abstract

Carbon-dioxide (CO<sub>2</sub>) is the main contributor to anthropogenic global warming, and the timing of its peak concentration in the atmosphere is likely to govern the timing of maximum radiative forcing. While dynamics of atmospheric CO<sub>2</sub> is governed by multiple time-constants, we idealize this by a single time-constant to consider some of the factors describing the time-delay between peaks in CO<sub>2</sub> emissions and concentrations. This time-delay can be understood as the time required to bring CO<sub>2</sub> emissions down from its peak to a small value, and is governed by the rate of decarbonization of economic activity. This decarbonization rate affects how rapidly emissions decline after having achieved their peak, and a rapid decline in emissions is essential for limiting peak radiative forcing. Long-term mitigation goals for CO<sub>2</sub> should therefore consider not only the timing of peak emissions, but also the rate of decarbonization. We discuss implications for mitigation of the fact that the emissions peak corresponds to small but nonzero emissions. One consequence is that the timing of peak CO<sub>2</sub> is not influenced by its atmospheric lifetime, despite its long lifetime being the origin of the delay in the concentration peak.

## 1 Introduction

As countries undertake voluntary commitments towards a new international climate treaty to be decided in 2015 (*UNFCCC* (2014a,b)), these will include mitigation of not only carbon-dioxide (CO<sub>2</sub>) but also other climate forcers (*UNFCCC* (2014c)). CO<sub>2</sub> is, and is likely to remain, the largest contribution to radiative forcing (*Forster et al.* (2007); *Myhre et al.* (2013)). Limiting long-term warming requires limiting the growth in global CO<sub>2</sub> emissions, and eventually reducing these emissions. If the present increasing trend in global CO<sub>2</sub> emissions is eventually reversed so that an emissions peak occurs, the corresponding peak in concentration will be delayed because of its long atmospheric lifetime (*Allen et al.* (2009); *Meinshausen et al.* (2009); *Mignone et al.* (2008)).

A CO<sub>2</sub> concentration peak would be a significant event for global climate: it would govern the maximum contribution of CO<sub>2</sub> emissions to radiative forcing. Furthermore, assuming that CO<sub>2</sub> continues to be the major contribution to radiative forcing, then its peak concentration will strongly influence the magnitude and timing of peak global warming.

The Earth's CO<sub>2</sub> cycle is complex, involving multiple reservoirs that maintain exchanges occurring at very different rates (*Archer et al. (1997); Cox et al. (2000); Falkowski et al. (2000)*). About three-fourths of excess CO<sub>2</sub> in the atmosphere gets absorbed relatively quickly via exchange with the ocean, within few centuries; while the rest requires many thousands of years in order to react with CaCO<sub>3</sub> or silicate rocks on land (*Archer et al. (1997); Archer and Brovkin (2008); Archer et al. (2009)*). Accurate characterization of the different processes that are involved, in order to describe the fate of excess atmospheric CO<sub>2</sub>, requires coupled climate-carbon-cycle or Earth-system models; such models have been employed to describe effects of emissions mitigation scenarios on CO<sub>2</sub> in the atmosphere (*Petoukhov et al. (2005); Friedlingstein et al. (2006)*). As the mitigation of CO<sub>2</sub> emissions unfolds, these and similar models will play important roles in estimating the consequences for atmospheric CO<sub>2</sub>, including the timing and magnitude of its peak concentration.

This paper solves a one-dimensional linear model of atmospheric CO<sub>2</sub> to understand the factors controlling the time-delay between peaks in emission and concentration. The model does not consider a number of complexities involved in the carbon cycle, such as nonlinear effects of surface-ocean saturation (*Caldeira and Casting (1993)*), the dynamics of the other CO<sub>2</sub> reservoirs leading to multiple time-constants for CO<sub>2</sub> uptake (*Archer et al. (1997)*), or effects of ocean circulation and biology (*Siegenthaler and Sarmiento (1993); Sarmiento et al. (1998)*); all of which would influence rates of CO<sub>2</sub> exchange between the atmosphere and these reservoirs. These limitations are significant, and preclude using the model here for prediction or decision-making. Previous studies have described the relationship between mitigation and warming, and highlighted the importance of rapid mitigation (for e.g. *Socolow and Lam (2007); Allen et al. (2009); Allen and Stocker (2014); Huntingford et al. (2012)*). Here we focus specifically on solving the model of atmospheric CO<sub>2</sub> analytically, to identify some of the important factors controlling the time to the concentration peak of CO<sub>2</sub>.

## 2 Models of emissions and carbon cycle

### 2.1 Carbon cycle model

The carbon-cycle model describes variation in concentration  $u(t)$  of CO<sub>2</sub>, with preindustrial equilibrium value denoted by  $u_p$ . Time  $t$  describes departure from the present, in years. The atmospheric reservoir of CO<sub>2</sub> is alone described, and rate of loss from this is assumed to depend linearly on  $u(t)$ . Dynamics can then be characterized in terms of effective e-folding time-constant  $\tau_u$ , and the rate of

change of concentration is

$$\dot{u}(t) \equiv \frac{du(t)}{dt} = m(t) - \frac{u(t) - u_p}{\tau_u} \quad (1)$$

where  $m(t)$  is anthropogenic emissions in concentration units, i.e. the rate of increase in concentration in the hypothetical case of infinite atmospheric lifetime. Concentration is noted in parts per million (ppm). Atmospheric emission of CO<sub>2</sub> in the year 2013 was  $36 \times 10^{12}$  kg, equivalent to 4.5 ppm.<sup>1</sup>

Equation (1) accounts for effects of natural exchange of CO<sub>2</sub> between the atmosphere and other reservoirs, which would drive the system to  $u(t) = u_p$  in the absence of anthropogenic emissions. The CO<sub>2</sub> present in excess of this value is what governs the loss from the atmosphere in this model.

## 2.2 Emissions model

Emissions is described as the product of two factors: gross global product (GGP)  $g(t)$  and emissions intensity  $\mu(t)$ . The GGP is assumed to increase at constant rate  $r$ , so that  $g(t) = g_0 e^{rt}$ . Emissions intensity is reduced in the model at an increasing rate, i.e.  $\mu(t) = \mu_0 e^{-\lambda(t)}$ , where  $\lambda(t)$  is an increasing function with  $\lambda(0) = 0$ . Hence emissions can be written as  $m(t) = m_0 e^{rt - \lambda(t)}$ . We choose the function  $\lambda(t) = kt^2$  with  $k > 0$ . We call parameter  $k$  the decarbonization rate, it represents the rate at which the reduction of CO<sub>2</sub> intensity of GGP is accelerated.

This nonlinearity of  $\lambda(t)$  leads to initial increase in emissions, followed by decrease. Peak in emissions occurs when  $dm(t)/dt = (r - 2kt)m(t) = 0$ , i.e. when  $t = r/2k$ .

The model represents a 2-parameter family of curves and in general cannot reproduce the Representative Concentration Pathways, developed for climate modeling experiments (*van Vuuren et al. (2011)*). However it can span a wide range of relevant radiative forcing values (Figure 2c).

## 3 Results

Figure 1 shows a sample trajectory of CO<sub>2</sub> emissions and corresponding concentrations reconstructed from (*Allen et al. (2009)*), and based on a carbon-cycle model. Concentrations for this emissions pathway obtained by integrating equation (1) are also shown. Results are shown for different values of the atmospheric lifetime of CO<sub>2</sub>. Clearly the model is an inadequate representation of the carbon-cycle. A very long lifetime is needed to reproduce the time to the peak concentration, whereas a short lifetime reproduces the value of the concentration peak. This indicates the presence of multiple e-folding time-constants in the atmospheric response of CO<sub>2</sub>, as is well known (for e.g. *Archer et al. (1997)*).

---

<sup>1</sup>If CO<sub>2</sub> had infinite lifetime, emissions in the year 2013 would have increased atmospheric concentration by 4.5 ppm.

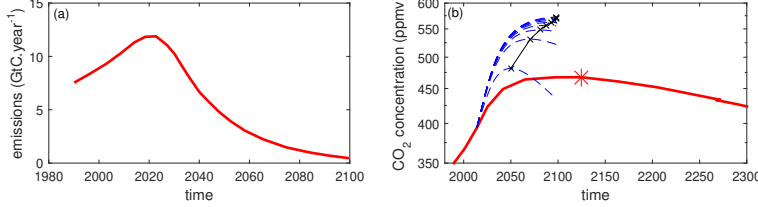


Figure 1: Test of one-dimensional model in equation (1): (a) a reconstructed emissions trajectory from Figure 1 of (Allen *et al.* (2009)); (b) corresponding concentration pathway reconstructed from (Allen *et al.* (2009)) in red, and solutions from integrating equation (1) for values of  $\tau_u$  ranging from 100 to 1700 years in blue. Peak concentration in the trajectory of (Allen *et al.* (2009)) is indicated by the asterisk and corresponding peak concentrations from equation (1) by the crosses. The one-dimensional model is an inadequate representation of the CO<sub>2</sub> cycle and the following results serve mainly as a thought-experiment.

### 3.1 Analytical solution for time-delay

Despite the considerable limitations of our model, it can be solved easily and this provides some indication of factors controlling the time-delay. We denote the time to the emissions peak as  $t_1$ , the time to the concentration peak as  $t_2$ , and the time-delay as  $\delta t \equiv t_2 - t_1$ . The model in equation (1) has been integrated analytically, in the Supplementary Information (SI). The exact solution for  $t_2$  is

$$t_2 = \tau_u \ln \frac{\dot{u}(0)}{\tau_u} + \left( \dot{m}_{av,i} - \dot{m}_{av,d} \right) e^{t_1/\tau_u} - \dot{m}_{av,i} \quad (2)$$

where  $\dot{u}(0)$  is the rate of increase in concentration at the present time, and  $\dot{m}_{av,i}$  and  $\dot{m}_{av,d}$  are average rates of increase in emissions during their growing and declining phases respectively, weighted by  $e^{t/\tau_u}$ , specifically

$$\dot{m}_{av,i} = \frac{1}{e^{t_1/\tau_u} - 1} \int_0^{t_1} e^{z/\tau_u} \frac{dm(z)}{dz} dz \quad (3)$$

and

$$\dot{m}_{av,d} = \frac{1}{e^{t_2/\tau_u} - e^{t_1/\tau_u}} \int_{t_1}^{t_2} e^{z/\tau_u} \frac{dm(z)}{dz} dz \quad (4)$$

so that  $\dot{m}_{av,i}$  is positive and  $\dot{m}_{av,d}$  is negative. Weighting by  $e^{t/\tau_u}$  in the equations above is essential to obtaining the exact solution. It turns out that we can closely approximate  $\dot{m}_{av,i}$  and  $\dot{m}_{av,d}$  by the actual rates

$$\dot{m}_i = \frac{1}{t_1} \int_0^{t_1} \frac{dm(z)}{dz} dz \quad (5)$$

and

$$\dot{m}_d = \frac{1}{t_2 - t_1} \int_{t_1}^{t_2} \frac{dm(z)}{dz} dz \quad (6)$$

which describe the average rates of change of emissions during their growing and declining phases respectively (as shown in Supplementary Information Figure 2). Hence we substitute the latter quantities in equation (2), yielding for the time-delay

$$\delta t \cong \tau_u \ln \frac{\frac{\dot{u}(0)}{\tau_u} + (\dot{m}_i - \dot{m}_d) e^{t_1/\tau_u} - \dot{m}_i}{-\dot{m}_d} - t_1 \quad (7)$$

In contrast to equation (2), this relationship is an approximation. The denominator in the logarithm of the above equation is positive, because  $\dot{m}_d$  is negative. Time-delay increases with the present growth rate of concentration  $\dot{u}(0)$ . It increases with the average rate of increase of emissions  $\dot{m}_i$  during its growth phase. A longer growth phase (i.e. larger  $t_1$ ) increases the time to peak concentrations (ref. equation (2)). Faster decrease of emissions in its declining phase (i.e. larger  $-\dot{m}_d$ ) reduces time-delay. Figure 3a verifies the approximation in equation (7). Plotted is the exact value of  $t_2$  from numerical integration and the estimate obtained by using equation (7). Across a wide range of emissions scenarios, varying the GGP growth rate and decarbonization rate, the approximation works reasonably well. Therefore we describe time-delay in terms of actual rates of change of emissions.

### 3.2 Effects of GGP growth rate and decarbonization rate

Given prior emissions profiles the model of equation (7) can be used to estimate the rates  $\dot{m}_i$  and  $\dot{m}_d$  and thereby the corresponding times to peak CO<sub>2</sub> concentration in the model. The model of emissions in Section 2.2 has been used to generate emissions profiles, but can also help us understand what controls these rates. Figure 2a plots the influence of GGP growth rate and decarbonization rate on  $\dot{m}_i$ . This growth rate of emissions is more sensitive to GGP growth rate, especially for large values of decarbonization rate  $k$ . In the SI, it is shown that for large  $k$  we can make the approximation that  $\dot{m}_i \cong rm_0/2$ , so the emissions growth rate increases linearly with the GGP growth rate but does not depend on the decarbonization rate. This is seen in the plot.

Figure 2b plots the influence of GGP growth rate and decarbonization rate on  $\dot{m}_d$ . During its declining phase, rate of change of emissions depends mainly on decarbonization rate  $k$ . A heuristic explanation is as follows. Emission peaks when the growth rate of GGP is canceled by the rate of decrease of emissions intensity. At later times the emissions intensity is decreasing faster and governs the rate of decrease of emissions. The absolute magnitude of rate  $\dot{m}_d$  increases rapidly with the decarbonization rate.

Figure 2c plots the peak in CO<sub>2</sub> radiative forcing that occurs at  $t_2$ , calculated as  $RF = 5.35 \log(u(t)/u_p)$ . GGP growth rate has negligible influence on peak radiative forcing in scenarios where the decarbonization rate is high, but the influence of economic growth increases if decarbonization is slow.

Figure 3b plots the time-delay between peak CO<sub>2</sub> emissions and concentrations, for different GGP growth rates and decarbonization rates. Shown are the exact solution from numerical integration and the approximations using

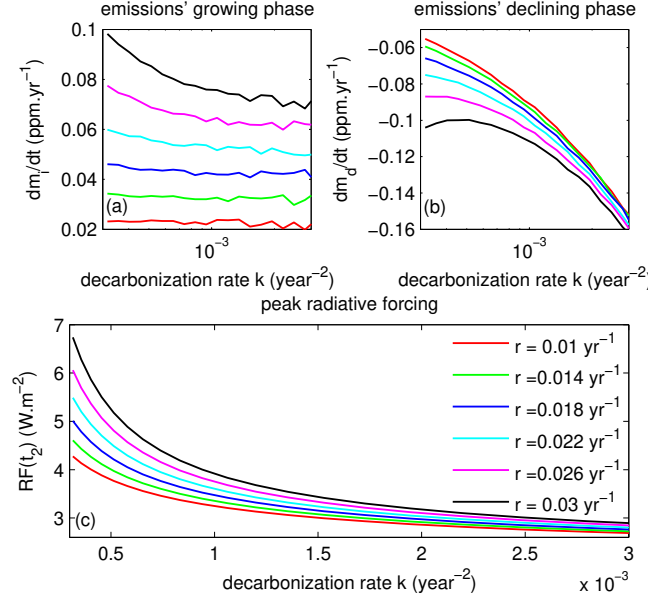


Figure 2: Effect of GGP growth rate  $r$  and decarbonization rate  $k$  on: (a) rate of change of emissions  $\dot{m}_i$  during its increasing phase between  $t = 0$  and  $t = t_1$ ; (b) rate of change of emissions  $\dot{m}_d$  between  $t = t_1$  and  $t = t_2$ ; (c) the peak in radiative forcing that occurs at  $t = t_2$ . During its increasing phase of emissions, the growth rate  $\dot{m}_i$  is more sensitive to the rate of GGP growth. When emissions are decreasing, the rate of change  $\dot{m}_d$  is sensitive mainly to the decarbonization rate.

equation (7). To a good approximation the time-delay depends only on the decarbonization rate and not on GGP growth rate. Nonlinear regression of  $\delta t$  versus  $k$  gave the relation  $\delta t = 2.3k^{-0.42}$ . The next section discusses why.

### 3.3 Interpretation of time-delay

Figure 4a plots wedge-shaped emissions profiles for three different scenarios. These scenarios all lead to complete decarbonization at  $t = 85$  years, and have the same cumulative emissions. The scenarios in Figure 4a differ in the time to peak emissions. Figure 4b shows corresponding concentration pathways for these scenarios. Peak concentrations are approximately the same for the different scenarios. Figure 4c helps understand this result, and interpret the time-delay. Shown in this panel are the emissions and, in the same plot, the excess concentration divided by atmospheric lifetime, i.e.  $(u(t) - u_p)/\tau_u$ . Following equation (1), this must equal emissions when  $\dot{u}(t) = 0$ , and therefore the intersection between corresponding curves gives the time to peak concentrations. Physically, the peak in concentration occurs when emissions become just small

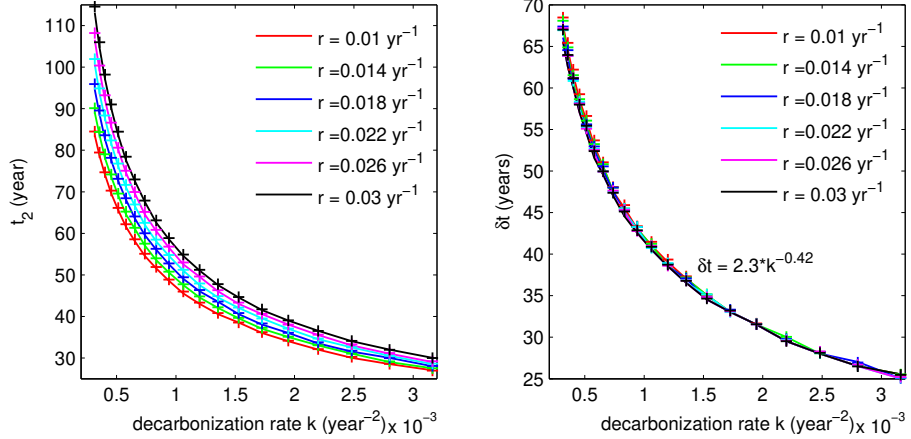


Figure 3: Effect of GGP growth rate  $r$  and decarbonization rate  $k$  on: (a) time  $t_2$  to peak concentrations; (b) time-delay  $\delta t$  between peak emission and concentration. Continuous lines show the exact solution and crosses indicate the approximation using equation (7). The approximation is accurate for wide ranges of  $r$  and  $k$ . The time-delay  $\delta t$  is approximately a function of only  $k$ . Nonlinear regression of  $\delta t$  versus  $k$  yields the relation  $\delta t = 2.3k^{-0.42}$ .

enough to be balanced by the rate of uptake of CO<sub>2</sub> from the atmosphere.

Because of the large atmospheric lifetime of CO<sub>2</sub>, the intersection in Figure 4c occurs when emissions are small. Because peak concentration occurs when emissions are small, the time to the corresponding peak concentration for the three scenarios is approximately the same. This time is close to when complete decarbonization occurs, and because cumulative CO<sub>2</sub> emissions are the same for the three emissions profiles, the peak concentrations are also approximately the same. Thereby the long atmospheric lifetime of CO<sub>2</sub> makes the peak concentration of CO<sub>2</sub> generally depend largely on the cumulative emissions up to the concentration peak. Contrast this with the cases shown in SI Figure 4 where, for the same emissions pathways but with a much lower atmospheric lifetime of 50 years, the time to peak concentration and these concentrations themselves differ considerably.

Previous authors have noted the importance of cumulative carbon emissions (*Allen et al. (2009); Zickfeld et al. (2009)*). With respect to maximum concentrations of CO<sub>2</sub>, the relevant cumulative emissions are up to the concentration peak at  $t_2$ , and this can of course differ across emissions scenarios that have the same total emissions. SI Figure 5 shows such a situation; in the scenarios considered there, the relevant window for calculating cumulative emissions differs significantly although total emissions are the same.

This interpretation of the time-delay allows us to suggest an explanation for the approximate power-law relationship between  $\delta t$  versus  $k$  in Figure 3b.

Emissions at  $t_2$  is

$$m(t_2) = m_0 e^{r(t_1+\delta t)-k(t_1+\delta t)^2} \quad (8)$$

and expanding the square in the exponent above and substituting  $t_1 = r/2k$  yields

$$m(t_2) = m_0 e^{r^2/4k} e^{-k(\delta t)^2} \quad (9)$$

Therefore the time required to bring emissions down to some critical value, say  $m_*$ , is given by

$$m_0 e^{r^2/4k} e^{-k(\delta t)^2} = m_* \quad (10)$$

The critical value  $m_*$  depends on excess concentration as  $(u(t_2) - u_p) / \tau_u$ , from equation (1). Excess concentration at  $t_p$  depends on cumulative emissions which, for large  $k$ , is

$$\int_0^{t_2} m(z) dz \cong \frac{m_0}{2} \sqrt{\frac{\pi}{k}} e^{r^2/4k} \quad (11)$$

(see SI Section 9). Therefore the condition for peak concentration is

$$m_0 e^{r^2/4k} e^{-k(\delta t)^2} = m_* \propto \frac{m_0}{2} \sqrt{\frac{\pi}{k}} e^{r^2/4k} \quad (12)$$

from which, finally

$$k(\delta t)^2 = c + \frac{1}{2} \log k \quad (13)$$

with some constant  $c$ . This shows that the time-delay depends only on the decarbonization rate. The decrease in the fitted exponent from 0.50 to 0.42 (as occurs in Figure 3b) must arise from the weak dependence on  $k$  in the right side of equation (13). See SI Section 9 for further details. In summary, growth rate of GGP does not influence the time-delay in the model because it has the same effect on emissions  $m(t_2)$  and the critical value of emissions  $m_*$ , so these effects cancel. This results from the quadratic form of  $\lambda(t)$ . In general if the approximations are  $g(t) = e^{(r_1+r_2t+o(t))t}$  and  $\mu(t) = \mu_0 e^{-(\lambda_1+\lambda_2t+o(t))t}$ , i.e. if emissions can be approximated as the exponential of a quadratic function in  $t$ , then the time-delay according to the model would depend only on the quadratic coefficient  $r_2 + \lambda_2$  of the exponent. In general this is not the case.

### 3.4 Insensitivity to atmospheric lifetime

The effective atmospheric lifetime of CO<sub>2</sub> is uncertain (*Archer* (2005); *Archer and Brovkin* (2008); *Archer et al.* (2009)). One implication of our interpretation of the time-delay is its insensitivity to atmospheric lifetime. This is not obvious from equation (7) but can be seen by making a further approximation. Considering only cases where  $t_1 \ll \tau_u$ , i.e. peak emission occurs on a time much shorter than the atmospheric lifetime, and where  $m(t_1) - m(0) \sim m(0)$ , i.e. the maximum increase in emissions is of the same magnitude as present emissions, then we can approximate

$$\delta t \cong \frac{\dot{u}(0) + (\dot{m}_i + \dot{m}_d) t_1}{-\dot{m}_d} \quad (14)$$

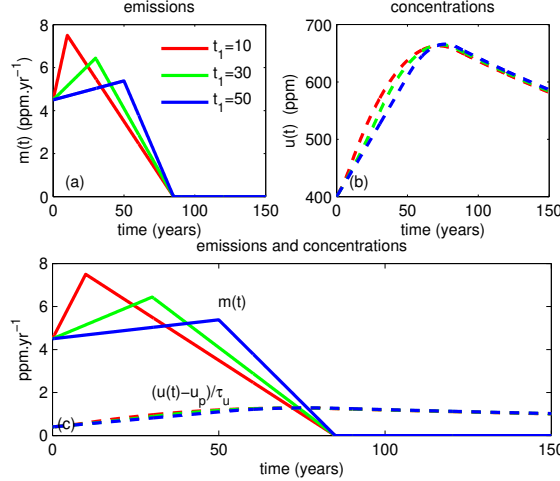


Figure 4: Three emissions scenarios reaching zero emissions in 2100 (i.e. at  $t = 85$  years) and each having the same cumulative emissions: (a) emissions profiles; (b) corresponding concentrations; (c) time to peak concentration as the intersection of  $m(t)$  and  $(u(t) - u_p) / \tau_u$ . For different scenarios obeying these constraints, the time at which peak concentration occurs is approximately the same:  $t_2$  for the three cases is 72.2, 74.0, and 76.7 years respectively.

which depends on atmospheric lifetime only through  $u(0)$  and the influence is weak (see SI for derivation). The reason for such a result is as follows. The time to peak concentrations is the time it takes to bring emissions down to a small value. The time it takes to bring emissions down to a given value does not depend on the atmospheric lifetime.

Of course this is only an approximation. Actually the critical value  $m_*$  depends slightly on the atmospheric lifetime and this influences the time to the concentration peak (see SI Section 9 for detailed calculations about the influence of  $\tau_u$  and other parameters on  $m_*$ ).

But the influence of  $\tau_u$  on the critical value  $m_*$  is small, compared to the magnitude of emissions reductions necessary. Therefore the value of  $\delta t$  is governed by the amount of time it takes to bring emissions down to a small value, and affected very little by small differences in the critical value. Figure 5 illustrates this. Shown is a single emissions profile, and corresponding curves of  $(u(t) - u_p) / \tau_u$  for three different values of the atmospheric lifetime. Time to peak concentration is given by the corresponding intersection with the emissions curve. Despite threefold differences in the atmospheric lifetime between these curves, the time to peak concentration of CO<sub>2</sub> varies by less than 1/3.

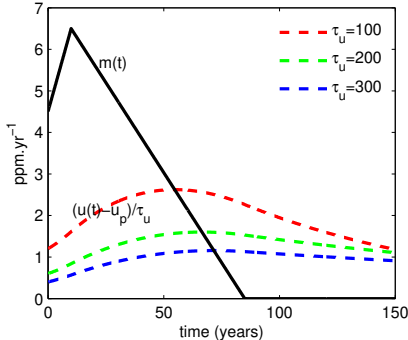


Figure 5: Effect of atmospheric lifetime of  $\text{CO}_2$  on the time to peak concentration. Shown are three curves for  $\tau_u$  of 100, 200, and 300 years; the corresponding values of  $t_2$  are 44.7, 56.5, and 61.7 years respectively.

## 4 Discussion

The one-dimensional linear model is not adequate to describe  $\text{CO}_2$  in the atmosphere, but it holds lessons that appear generic to more realistic models. The peak in  $\text{CO}_2$  concentrations occurs when emissions have reached a small value. The additional time to the peak concentration is the time necessary to bring emissions down from its peak to this critical value. The critical value depends on the excess concentration of  $\text{CO}_2$  in the atmosphere compared to the preindustrial situation. Growth rate of GGP has similar effects on the emissions at any future time as it does on the critical value below which emissions must be reduced at the time of the concentration peak. Therefore the time-delay between peak emissions and concentration is not influenced by this growth rate of GGP, and depends only on the rate of decarbonization. This result is exact for the emissions model considered here, with its exponent a quadratic function of time, but the intuition behind it appears to be more generally valid. The rate of decarbonization primarily influences the rate at which  $\text{CO}_2$  emissions are reduced following their peak.

Uncertainty in the atmospheric lifetime of  $\text{CO}_2$  has little effect on the timing of the concentration peak. While the value of the atmospheric lifetime affects the critical emissions below which the peak in concentration occurs, this critical value is necessarily small. Consequently the timing is governed by the time required to bring emissions down to a small value, and is hardly affected by small differences in the critical value. The crucial phenomenon here is that despite uncertainties in  $\text{CO}_2$  lifetime, this lifetime is large.

More generally the small but nonzero emissions that corresponds to the emissions peak has implications for mitigation. It is not sufficient to achieve an early peak in  $\text{CO}_2$  emissions. It is equally important to reduce emissions rapidly, by decarbonizing the global economy. Cumulative emissions until the concentration peak occurs are a good measure of the consequences for the maximum radiative

forcing from CO<sub>2</sub>. These can differ significantly from total emissions across time, and this has consequences for comparing across mitigation scenarios.

The model presented here is very simple, and does not consider nonlinear effects arising from saturation of the surface oceans with CO<sub>2</sub>, effects of ocean circulation and biology, or the dynamics of other reservoirs besides the atmosphere. While considering these effects might introduce additional factors relevant to this discussion, it does not appear that these will affect the interpretation of the time-delay or implications for policy discussed here. However it would be necessary to examine the influence of multiple time-constants of atmospheric CO<sub>2</sub> on these results.

## Acknowledgments

This research has been supported by Divecha Centre for Climate Change, Indian Institute of Science. The author thanks G Bala and J Srinivasan for helpful discussion.

## References

Allen, M. R., and T. F. Stocker (2014), Impact of delay in reducing carbon dioxide emissions, *Nature Climate Change*, 4, 23–26, doi:<http://dx.doi.org/10.1038/nclimate2077>.

Allen, M. R., D. J. Frame, C. Huntingford, C. D. Jones, J. A. Lowe, M. Meinshausen, and N. Meinshausen (2009), Warming caused by cumulative carbon emissions towards the trillionth tonne, *Nature*, 458, 1163–1166, doi: <http://dx.doi.org/10.1038/nature08019>.

Archer, D. (2005), Fate of fossil-fuel CO<sub>2</sub> in geologic time, *Journal of Geophysical Research*, 110, C09S05, doi:<http://dx.doi.org/10.1029/2004JC002625>.

Archer, D., and V. Brovkin (2008), The millennial atmospheric lifetime of anthropogenic CO<sub>2</sub>, *Climatic Change*, 90(3), 283–297, doi:<http://dx.doi.org/10.1007/s10584-008-9413-1>.

Archer, D., H. Kheshgi, and E. Maier-Reimer (1997), Multiple timescales for neutralization of fossil fuel CO<sub>2</sub>, *Geophysical Research Letters*, 24, 405–408, doi:<http://dx.doi.org/10.1029/97GL00168>.

Archer, D., M. Eby, V. Brovkin, A. Ridgwell, and L. Cao (2009), Atmospheric lifetime of fossil fuel carbon dioxide, *Annual Review of Earth and Planetary Sciences*, 37, 117–134, doi:<http://dx.doi.org/10.1146/annurev.earth.031208.100206>.

Caldeira, K., and J. F. Casting (1993), Insensitivity of global warming potentials to carbon dioxide emission scenarios, *Nature*, 366, 251–253, doi:<http://dx.doi.org/10.1038/366251a0>.

Cox, P. M., R. A. Bett, C. D. Jones, S. A. Spall, and I. J. Totterdell (2000), Acceleration of global warming due to carbon-cycle feedbacks in a coupled climate model, *Nature*, *408*, 184–187, doi:<http://dx.doi.org/10.1038/35041539>.

Falkowski, P., R. J. Scholes, E. Boyle, J. Canadell, D. Canfield, J. Elser, N. Gruber, K. Hibbard, P. Hogberg, S. Linder, F. T. Mackenzie, B. M. III, T. Pedersen, Y. Rosenthal, S. Seitzinger, V. Smetacek, and W. Steffen (2000), The global carbon cycle: A test of our knowledge of Earth as a system, *Science*, *290*, 291–296, doi:<http://dx.doi.org/10.1126/science.290.5490.291>.

Forster, P., V. Ramaswamy, P. Artaxo, T. Berntsen, R. Betts, and D. Fahey (2007), *Climate Change 2007: The Physical Science Basis. Contribution of Working Group I to the Fourth Assessment Report of the Intergovernmental Panel on Climate Change*, chap. Changes in Atmospheric Constituents and in Radiative Forcing, Cambridge University Press.

Friedlingstein, P., P. Cox, R. Betts, L. Bopp, W. von Bloh, V. Brovkin, P. Cadule, S. Doney, M. Eby, and I. Fung (2006), Climate-carbon cycle feedback analysis: Results from the C4MIP Model Intercomparison, *Journal of Climate*, *19*, 3337–3353, doi:<http://dx.doi.org/10.1175/JCLI3800.1>.

Huntingford, C., J. A. Lowe, L. K. Gohar, N. H. A. Bowerman, M. R. Allen, S. C. B. Raper, and S. M. Smith (2012), The link between a global 2C warming threshold and emissions in years 2020, 2050 and beyond, *Environmental Research Letters*, *7*, 1–8, doi:<http://dx.doi.org/10.1088/1748-9326/7/1/014039>.

Meinshausen, M., N. Meinshausen, W. Hare, S. C. B. Raper, K. Frieler, R. Knutti, D. J. Frame, and M. R. Allen (2009), Greenhouse-gas emission targets for limiting global warming to 2 C, *Nature*, *458*, 1158–1162, doi: <http://dx.doi.org/10.1038/nature08017>.

Mignone, B. K., R. H. Socolow, J. L. Sarmiento, and M. Oppenheimer (2008), Atmospheric stabilization and the timing of carbon mitigation, *Climatic Change*, *88*, 251–265, doi:<http://dx.doi.org/10.1007/s10584-007-9391-8>.

Myhre, G., D. Shindell, F. M. Breon, W. Collins, J. Fuglestvedt, and J. Huang (2013), *Climate Change 2013: The Physical Science Basis. Contribution of Working Group I to the Fifth Assessment Report of the Intergovernmental Panel on Climate Change*, chap. Anthropogenic and Natural Radiative Forcing, pp. 659–740, Cambridge University Press.

Petoukhov, V., M. Claussen, A. Berger, M. Crucifix, M. Eby, A. V. Eliseev, T. Fichefet, A. Ganopolski, H. Goosse, and I. Kamenkovich (2005), EMIC intercomparison project (EMIP-CO<sub>2</sub>): comparative analysis of EMIC simulations of climate, and of equilibrium and transient responses to atmospheric CO<sub>2</sub> doubling, *Climate Dynamics*, *25*, 363–385, doi:<http://dx.doi.org/10.1007/s00382-005-0042-3>.

Sarmiento, J. L., T. M. C. Hughes, R. J. Stouffer, and S. Manabe (1998), Simulated response of the ocean carbon cycle to anthropogenic climate warming, *Nature*, 393, 245–249, doi:<http://dx.doi.org/10.1038/30455>.

Siegenthaler, U., and J. L. Sarmiento (1993), Atmospheric carbon dioxide and the ocean, *Nature*, 365, 119–125, doi:<http://dx.doi.org/10.1038/365119a0>.

Socolow, R. H., and S. H. Lam (2007), Good enough tools for global warming policy making, *Philosophical Transactions of the Royal Society of London A*, 365, 897–934, doi:[10.1098/rsta.2006.1961](https://doi.org/10.1098/rsta.2006.1961).

UNFCCC (2014a), Lima call for climate action.

UNFCCC (2014b), Lima call for climate action puts world on track to Paris 2015.

UNFCCC (2014c), UNEP says IPCC report requires bold Paris pact.

van Vuuren, D. P., J. Edmonds, M. Kainuma, K. Riahi, A. Thomson, and K. Hibbard (2011), The representative concentration pathways: an overview, *Climatic Change*, 109, 5–31, doi:<http://dx.doi.org/10.1007/s10584-011-0148-z>.

Zickfeld, K., M. Eby, H. D. Matthews, and A. J. Weaver (2009), Setting cumulative emissions targets to reduce the risk of dangerous climate change, *Proceedings of the National Academy of Sciences of the United States of America*, 106, 16,129–16,134, doi:<http://dx.doi.org/10.1073/pnas.0805800106>.

# Supplementary Information for "Decarbonization and the time-delay between peak CO<sub>2</sub> emissions and concentrations"

## 1 Emissions model

Emissions is represented as the product of two factors: gross global product (GGP)  $g(t)$  and emissions intensity  $\mu(t)$ . GGP increases at constant rate  $r$  in the model, so that  $g(t) = g_0 e^{rt}$ . Emissions intensity decreases nonlinearly, i.e.  $\mu(t) = \mu_0 e^{-\lambda(t)}$ , where  $\lambda(t)$  is an increasing nonlinear function with  $\lambda(0) = 0$ . Hence emissions is  $m(t) = m_0 e^{rt - \lambda(t)}$ . We choose  $\lambda(t) = kt^2$  with  $k > 0$ . The nonlinearity of  $\lambda(t)$  leads to initial increase in emissions, followed by decrease. Peak emissions occurs when  $dm(t)/dt = (r - 2kt)m(t) = 0$ , i.e. when  $t = r/2k$ . We call parameter  $k$  the decarbonization rate, it represents the rate at which the reduction of CO<sub>2</sub> intensity of economic activity is accelerated.

## 2 Estimate of time-delay between peak emissions and concentrations

We consider a model of atmospheric concentration  $u(t)$  of a species, whose excess from its preindustrial value  $u_p$  decays linearly. Restricting ourselves to a one-dimensional model describing the atmospheric reservoir, the concentration in the model depends on a single atmospheric lifetime  $\tau_u$ . Then its rate of change is

$$\dot{u}(t) \equiv \frac{du(t)}{dt} = m(t) - \frac{u(t) - u_p}{\tau_u} \quad (1)$$

where  $m(t)$  is emissions in concentration units. In case of zero emission, this model has equilibrium  $u(t) = u_p$ . Before integration we rescale time, with  $s \equiv t/\tau_u$ , to make calculations more transparent. Denoting derivatives with respect to  $s$  by primes, we obtain

$$u'(s) \equiv \frac{du(s)}{ds} = \tau_u m(s) - u(s) + u_p \quad (2)$$

which is integrated to yield the solution

$$u(s) = e^{-s} u(0) + \tau_u e^{-s} \int_0^s e^z m(z) dz + u_p (1 - e^{-s}) \quad (3)$$

whose rate of change with respect to  $s$  is

$$u'(s) = -e^{-s}u(0) - \tau_u e^{-s} \int_0^s e^z m(z) dz + \tau_u m(s) + u_p e^{-s} \quad (4)$$

We denote the time where peak in emissions occurs at  $s = s_1$  and the time to the corresponding concentration peak as  $s = s_2$ . At the concentration peak,  $u'(s_2) = 0$ . From this and equation (4)

$$e^{-s_2} \frac{u(0) - u_p}{\tau_u} = m(s_2) - e^{-s_2} \int_0^{s_2} e^z m(z) dz \quad (5)$$

To study what influences  $s_2$ , we evaluate the integral in the right side using integration by parts

$$\int_0^{s_2} e^z m(z) dz = e^{s_2} m(s_2) - m(0) - \int_0^{s_2} e^z \frac{dm(z)}{dz} dz \quad (6)$$

and substitution of equation (6) into equation (5) followed by simplification yields

$$\frac{u(0) - u_p}{\tau_u} - m(0) = \int_0^{s_2} e^z \frac{dm(z)}{dz} dz \quad (7)$$

The left side is  $-u'(0)/\tau_u$ . The right side is decomposed into the sum of two integrals

$$\int_0^{s_2} e^z \frac{dm(z)}{dz} dz = \int_0^{s_1} e^z \frac{dm(z)}{dz} dz + \int_{s_1}^{s_2} e^z \frac{dm(z)}{dz} dz \quad (8)$$

Next, we define the weighted average rate of change of emissions between  $s = 0$  and  $s = s_1$  by

$$\int_0^{s_1} e^z \frac{dm(z)}{dz} dz \equiv m'_{av,i} \int_0^{s_1} e^z dz \quad (9)$$

with  $m'_{av,i} > 0$ . Likewise

$$\int_{s_1}^{s_2} e^z \frac{dm(z)}{dz} dz \equiv m'_{av,d} \int_{s_1}^{s_2} e^z dz \quad (10)$$

with  $m'_{av,d} < 0$ . Equations (9) and (10) involve weighting by  $e^z$  in the integral, so later times are weighted more. Substituting equations (8)-(10) into equation (7) and simplifying yields

$$s_2 = \ln \frac{\frac{u'(0)}{\tau_u} + (m'_{av,i} - m'_{av,d}) e^{s_1} - m'_{av,i}}{-m'_{av,d}} \quad (11)$$

Returning to the representation in terms of actual time  $t$  (in years), and using  $s_2 = t_2/\tau_u$ ,  $u'(t) = \tau_u \dot{u}(t)$ , and  $m'(t) = \tau_u \dot{m}(t)$  gives

$$t_2 = \tau_u \ln \frac{\frac{\dot{u}(0)}{\tau_u} + (\dot{m}_{av,i} - \dot{m}_{av,d}) e^{t_1/\tau_u} - \dot{m}_{av,i}}{-\dot{m}_{av,d}} \quad (12)$$

so that the delay  $\delta t \equiv t_2 - t_1$  is

$$\delta t = \tau_u \ln \frac{\frac{\dot{u}(0)}{\tau_u} + (\dot{m}_{av,i} - \dot{m}_{av,d}) e^{t_1/\tau_u} - \dot{m}_{av,i}}{-\dot{m}_{av,d}} - t_1 \quad (13)$$

Let us consider the case where  $t_1 \ll \tau_u$ , i.e. where peak emissions occurs within a period much shorter than atmospheric lifetime. Then, using the series approximation for  $e^x$  to 1<sup>st</sup> degree in  $x$ , i.e.  $e^x \cong 1 + x$ , we obtain

$$\delta t \cong \tau_u \ln \frac{-\dot{m}_{av,d} + \frac{\dot{u}(0)}{\tau_u} + \frac{t_1}{\tau_u} \dot{m}_{av,i}}{-\dot{m}_{av,d}} - t_1 \quad (14)$$

If  $\dot{m}_{av,i}$  and  $\dot{m}_{av,d}$  are comparable in magnitude and with  $t_1 \ll \tau_u$ , then  $(t_1/\tau_u) \dot{m}_{av,i} \ll -\dot{m}_{av,d}$ . Furthermore  $\dot{u}(0)/\tau_u < m(0)/\tau_u$  from equation (1); and if  $m(t_1) - m(0) \sim m(0)$ , i.e. the maximum increase in emissions is of the same rough magnitude as present emissions, then we also have  $\dot{u}(0)/\tau_u \ll -\dot{m}_{av,d}$ . Hence in the numerator of equation (14),  $-\dot{m}_{av,d}$  is the dominant term. Using the series approximation for  $\ln(1 + x)$  to 1<sup>st</sup> degree in  $x$ , i.e.  $\ln(1 + x) \cong x$ , we obtain

$$\delta t \cong \frac{\dot{u}(0) + (\dot{m}_{av,i} + \dot{m}_{av,d}) t_1}{-\dot{m}_{av,d}} \quad (15)$$

This increases with  $\dot{u}(0)$ , the rate of growth in present concentrations. It increases with  $\dot{m}_{av,i}$ , so quicker growth of emissions during its increasing phase increases the delay. It decreases with  $-\dot{m}_{av,d}$ , so rapid decrease in emissions following its peak reduces the delay. The effect of increasing  $t_1$ , i.e. the time to peak emissions, depends on the sign of  $\dot{m}_{av,i} + \dot{m}_{av,d}$ . Where this is positive, the delay increases with the time to peak emissions.

### 3 Verification of expressions for time-delay

SI Figure 1 plots the values of  $\delta t$  for the exact solution (calculated by numerical integration of equation (1)) along with the values calculated using equations (13) and (15) respectively. These are plotted for different values of the decarbonization rate  $k$ . The results of equation (13) are exact, but the approximation of equation (15) underestimates slightly, especially for longer delays where the ratio  $\delta t/\tau_u$  increases. The close correspondence between the three curves verifies these expressions.

### 4 Relation with actual rates of change of emissions

The expressions for time-delay were derived using the average rates of change of emissions, weighted by  $e^{t/\tau_u}$ . To see the relation with actual rates of change,

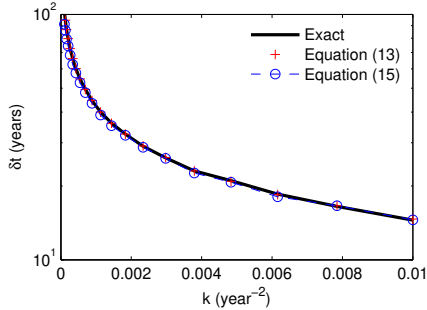


Figure 1: Time-delay  $\delta t$  versus decarbonization rate  $k$ . Shown are the exact solution and the results from equation (13) and equation (15). The parameters used are growth rate of GGP  $r = 0.01$  and  $\tau_u = 300$  years.

we consider the variables

$$\dot{m}_i = \frac{1}{t_1} \int_0^{t_1} \frac{dm(z)}{dz} dz \quad (16)$$

and

$$\dot{m}_d = \frac{1}{t_2 - t_1} \int_{t_1}^{t_2} \frac{dm(z)}{dz} dz \quad (17)$$

SI Figure 2 plots the weighted rates of change  $\dot{m}_{av,i}$  and  $\dot{m}_{av,d}$  defined in equations (9) and (10), and unweighted rates of change  $\dot{m}_i$  and  $\dot{m}_d$ , for different values of GGP growth rate and decarbonization rate. The actual (i.e. unweighted) rates of change closely approximate the weighted rates of change. Hence we can approximate the weighted rates in equations (13) and (15) by the actual rates of change of emissions.

## 5 Influence of $r$ and $k$ on $\dot{m}_i$ and $\dot{m}_d$

The rates of change of emissions have been defined in equations (16) and (17). We describe their relation with GGP growth rate  $r$  and decarbonization rate  $k$  in the emissions model. SI Figure 2 suggests that  $\dot{m}_i$  depends on both parameters, whereas  $\dot{m}_d$  is governed by the value of  $k$ .

Considering  $\dot{m}_i$ , it simplifies to

$$\dot{m}_i = \frac{1}{t_1} (m(t_1) - m(0)) \quad (18)$$

which can be written as

$$\dot{m}_i = \frac{m_0}{t_1} \left( e^{rt_1 - kt_1^2} - 1 \right) \quad (19)$$

and substituting  $t_1 = r/2k$  we obtain

$$\dot{m}_i = \frac{2km_0}{r} \left( e^{r^2/4k} - 1 \right) \quad (20)$$

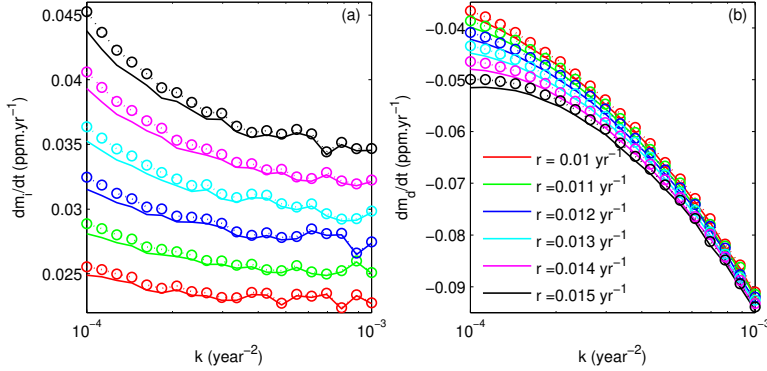


Figure 2: Average rates of change of emissions during its increasing and decreasing phases: (a) rate of change during its growing phase between  $t = 0$  and  $t = t_1$ ; (b) rate of change during the declining phase between  $t = t_1$  and  $t = t_2$ . Each curve plots results for a different value of GGP growth rate  $r$ . Continuous lines plot weighted rates of change  $\dot{m}_{av,i}$  and  $\dot{m}_{av,d}$ , and open circles indicate corresponding unweighted rates  $\dot{m}_i$  and  $\dot{m}_d$ . Unweighted rates of change approximate well the corresponding weighted rates of change.

If  $r^2/4k \ll 1$  the above expression simplifies to

$$\dot{m}_i \simeq \frac{rm_0}{2} \quad (21)$$

so that the average rate of change of emissions during its growth phase depends only on present emissions and the growth rate of GGP. For example with  $r = 0.01$  and  $k = 0.001$  this condition is satisfied. The relationship in equation (21) is seen in Figure 2a; for large values of  $k$  around 0.001 the value of  $\dot{m}_i$  does not depend on  $k$  but increases linearly with  $r$ .

Writing  $\alpha = r^2/4k$ , the series-solution for  $\dot{m}_i$  is

$$\dot{m}_i = \frac{rm_0}{2} \left( 1 + \frac{\alpha}{2} + \frac{\alpha^2}{6} + \frac{\alpha^3}{24} + \dots \right) \quad (22)$$

so in general it depends on both GGP growth rate and the decarbonization rate, increasing with  $\alpha$ .

By contrast  $\dot{m}_d$  is sensitive mainly to decarbonization rate  $k$ . This can be seen directly from Figure 2.

## 6 Peak radiative forcing from CO<sub>2</sub>

Here we describe the influence of  $r$  and  $k$  on the magnitude of the peak in radiative forcing from CO<sub>2</sub>. Radiative forcing is calculated using the formula  $RF(CO_2) = 5.35 \log(u/u_p)$ . This is plotted in SI Figure 3. Rate of GGP growth has negligible influence on peak radiative forcing in case of rapid decarbonization, but its effect is larger in case decarbonization is slow.

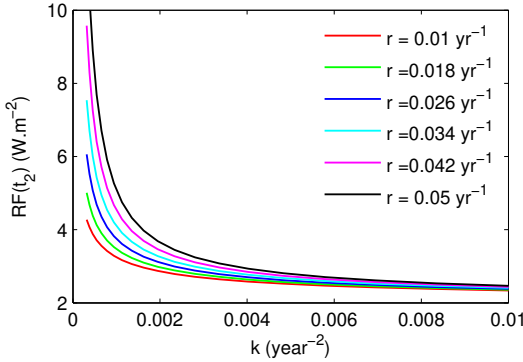


Figure 3: Peak radiative forcing  $RF(t_2)$  as a function of decarbonization rate  $k$  for different values of  $r$ .

## 7 Effect of atmospheric lifetime

SI Figure 4 plots a hypothetical (but unreal for the case of  $\text{CO}_2$ ) case where atmospheric lifetime is made relatively small  $\tau_u = 50$  years. Shown are emissions, concentrations, and the intersection between  $m(t)$  and  $(u(t) - u_p) / \tau_u$  for three different emissions scenarios reaching zero emissions in 2100 (i.e. at  $t = 85$  years) with each scenario having the same cumulative emissions. Contrary to the case of the result in the paper (paper Figure 4) with much larger atmospheric lifetime ( $\tau_u = 300$  years), where the time to peak concentration and peak concentrations are similar across these scenarios, here (in SI Fig. 4) the differences are larger. The contrast between the cases of Paper Fig. 4 and SI Fig. 4 reinforces the point that: the long atmospheric lifetime of  $\text{CO}_2$  causes its peak concentration to depend on the cumulative emissions.

## 8 Effect of the time to zero emissions

SI Figure 5 plots a case where atmospheric lifetime is  $\tau_u = 300$  years. Shown are emissions, concentrations, and the intersection between  $m(t)$  and  $(u(t) - u_p) / \tau_u$  for three different emissions scenarios reaching zero emissions at different times. Cumulative emissions are the same for the three scenarios. Despite this the peak concentration differs across these scenarios, because low emissions are reached at different times and hence the relevant window for computing cumulative emissions also differs.

## 9 Time-delay as a function of $r$ and $k$

We estimate the time-delay between peak emissions and concentration as a function of  $r$  and  $k$ . From equation (4) and  $u'(s_2) = 0$  are obtained the condition

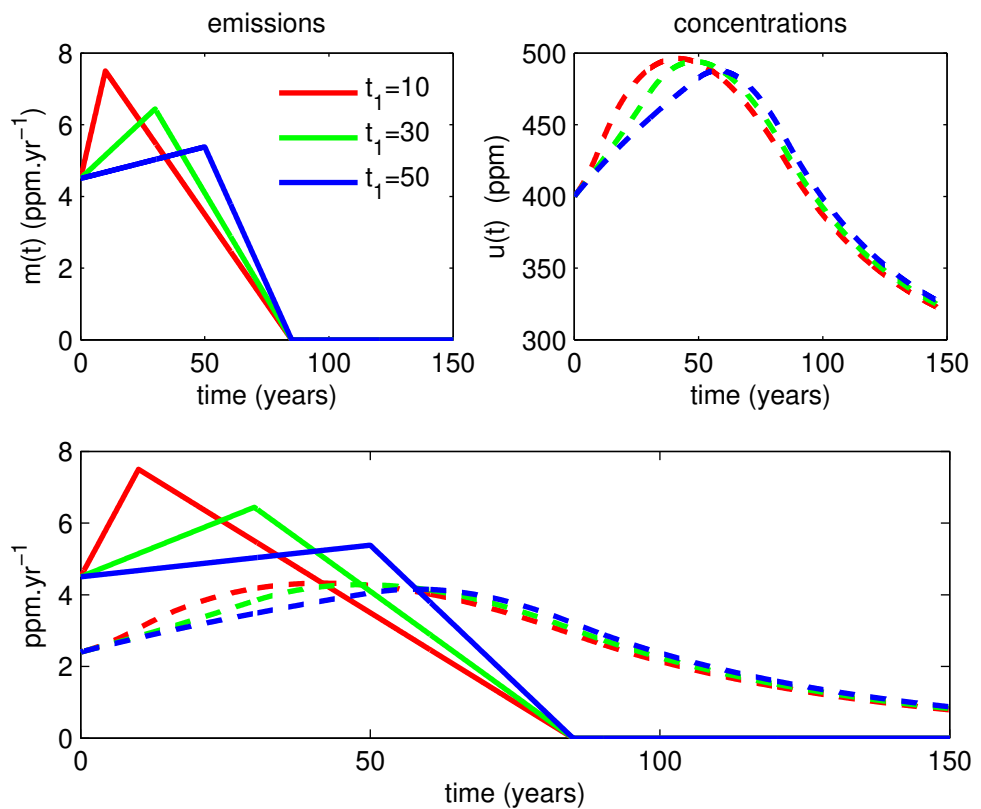


Figure 4: Three emissions scenarios reaching zero emissions in 2100 (i.e. at  $t = 85$  years) and each having the same cumulative emissions. Atmospheric lifetime in these simulations is taken to be  $\tau_u = 50$  years. In this case the time to peak concentration  $t_2$  for the three cases differs considerably: 41.7, 48.5, and 58.0 years respectively. Peak concentration is also different across these three scenarios.

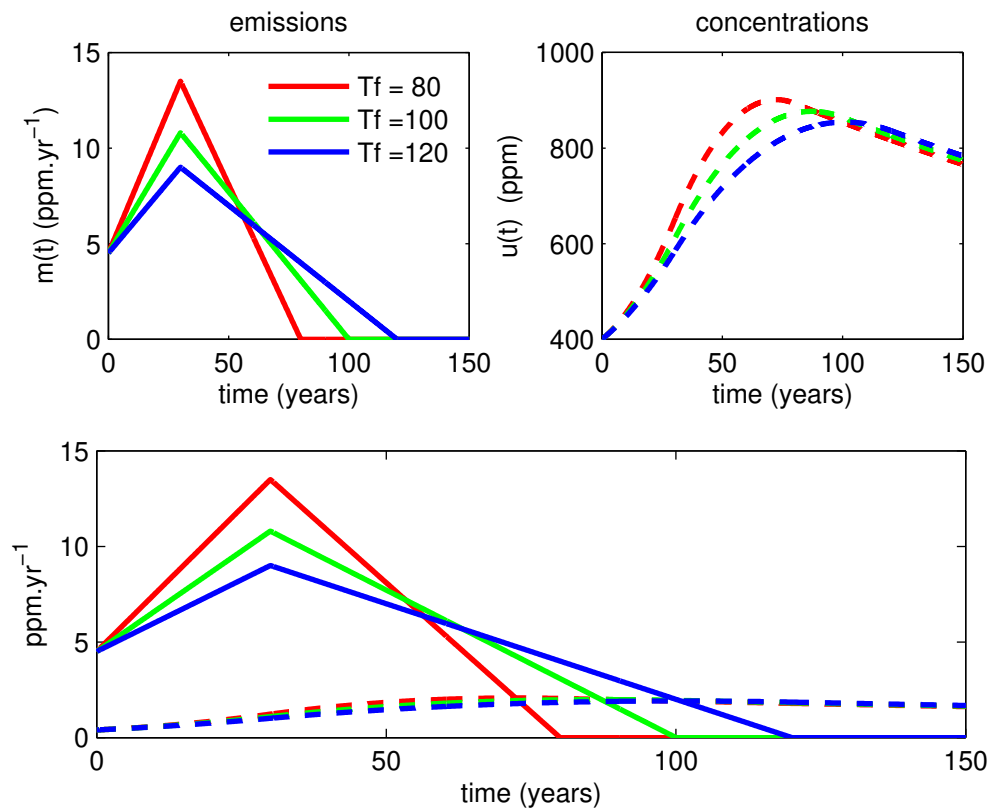


Figure 5: Three emissions scenarios reaching zero emissions in 2095, 2115, and 2135 respectively and each having the same cumulative emissions. Atmospheric lifetime in these simulations is taken to be  $\tau_u = 300$  years. In this case the time to peak concentration  $t_2$  for the three cases differs considerably: 72.3, 87.0, and 100.8 years respectively. The relevant cumulative emissions and correspondingly the peak concentration also differ.

for peak in concentration at  $t_2$

$$e^{-t_2/\tau_u} \frac{u(0) - u_p}{\tau_u} = m(t_2) - \frac{1}{\tau_u} e^{-t_2/\tau_u} \int_0^{t_2} e^{z/\tau_u} m(z) dz \quad (23)$$

Approximating the integral  $\int_0^{t_2} e^{z/\tau_u} m(z) dz$  by  $e^{t_2/\tau_u} \int_0^{t_2} m(z) dz$  this simplifies to

$$e^{-t_2/\tau_u} \frac{u(0) - u_p}{\tau_u} \cong m(t_2) - \frac{1}{\tau_u} \int_0^{t_2} m(z) dz \quad (24)$$

The condition for peak concentration is then as follows: the difference between emissions at  $t_2$  and cumulative emissions between  $t = 0$  and  $t_2$ , when divided by  $\tau_u$ , must be the small value on the left side of equation (24). With  $m(z) = m_0 e^{rz - kz^2}$ , we obtain the cumulative emissions

$$\int_0^{t_2} m(z) dz = \frac{m_0}{2} \sqrt{\frac{\pi}{k}} e^{r^2/4k} \left( \operatorname{erf} \left( \frac{r}{2\sqrt{k}} \right) - \operatorname{erf} \left( \frac{r - 2kt_2}{2\sqrt{k}} \right) \right) \quad (25)$$

where

$$\operatorname{erf}(x) = \frac{2}{\sqrt{\pi}} \int_0^x e^{-t^2} dt \quad (26)$$

is the error function. Let us consider large values of  $k$  for which  $\sqrt{kt_2} \sim 1$  and  $r < 2\sqrt{k}$ . Using the Taylor series expansion for  $\operatorname{erf}(x)$  to first-order in  $x$  for small  $x$ , cumulative emissions is approximated as

$$\int_0^{t_2} m(z) dz \cong \frac{m_0}{2} \sqrt{\frac{\pi}{k}} e^{r^2/4k} \left( 1 - \frac{r}{\sqrt{\pi k}} \right) \quad (27)$$

Then equation (24) becomes

$$e^{-t_2/\tau_u} \frac{u(0) - u_p}{\tau_u} \cong m(t_2) - \frac{1}{\tau_u} \frac{m_0}{2} \sqrt{\frac{\pi}{k}} e^{r^2/4k} \left( 1 - \frac{r}{\sqrt{\pi k}} \right) \quad (28)$$

The condition for peak concentrations is: the difference on the right side of equation (28) must become sufficiently small. How small depends on the initial disequilibrium, measured by the left side. Emissions at time  $t_2$  is

$$m(t_2) = m_0 e^{r(t_1 + \delta t) - k(t_1 + \delta t)^2} \quad (29)$$

Expanding the square in the exponent above and substituting  $t_1 = r/2k$  yields

$$m(t_2) = m_0 e^{r^2/4k} e^{-k(\delta t)^2} \quad (30)$$

Substituting equation (30) into equation (28) gives

$$e^{-k(\delta t)^2} = \frac{1}{\tau_u} \sqrt{\frac{\pi}{k}} \left( 1 - \frac{r}{\sqrt{\pi k}} \right) + e^{-t_2/\tau_u} e^{-r^2/4k} \frac{u(0) - u_p}{\tau_u m_0} \quad (31)$$

To simplify matters we consider large  $k$ . Correspondingly we can assume that  $e^{-t_2/\tau_u} \cong 1$  and  $e^{-r^2/4k} \cong 1$ . Furthermore for large  $k$ ,  $r/\sqrt{\pi k} \ll 1$ . Hence we obtain finally

$$\delta t \cong \left\{ -\log \left( \frac{1}{\tau_u} \sqrt{\frac{\pi}{k}} + \frac{u(0) - u_p}{\tau_u m_0} \right) \right\}^{1/2} k^{-1/2} \quad (32)$$

verifying two general features of the relationship between  $\delta t$  and the emissions model's parameters: a)  $\delta t$  is not sensitive to the value of GGP growth rate; b) there is approximately an inverse-square root dependence on  $k$ .